

Supplementary material for “The role of heatwave events on the occurrence and persistence of thermal stratification in the southern North Sea”

Wei Chen¹, Joanna Staneva¹, Sebastian Grayek¹, Johannes Schulz-Stellenfleth¹, and Jens Greinert²

¹Institute of Coastal Systems-Analysis and Modelling, Helmholtz-Zentrum Hereon, Max-Planck-Str. 1, 21502 Geesthacht, Germany

²GEOMAR Helmholtz Center for Ocean Research Kiel, Wischhofstr. 1-3, 24148 Kiel, Germany

Correspondence: Wei Chen (wei.chen@hereon.de)

1 Results of uncoupled NEMO model run

Figure S1 is similar to Figure 3 in the main text but shows the model run that uncoupled with the wave model WAM. Compared to the coupled model run, the water was colder near the bottom in the uncoupled run. For relatively deeper locations, e.g., the Dogger Bank and NSB III, the uncoupled model run can represent a water temperature closer to the observations than can the 5 coupled model run. However, it is worth noting that this does not mean that the uncoupled model performs better in predicting temperature profiles in the North Sea. Further analysis of the multiple-year water temperatures of the uncoupled model run revealed that without considering the wave effect, the simulation generally underestimated the near-bottom temperatures by 2 ~ 3°C during the warming period. This subsequently leads to a stronger stratification. As shown in Figure S1, the uncoupled model failed to represent the temperature profiles at FINO-1. It yielded a much larger vertical variance in water temperatures.

10 We compared the model results within the area between the south of 50 m isobath and 3-8°E. For this, data at the Dogger Bank and the MARNET station NSB III were used. The interannual variation in the seawater temperatures at the two stations was similar to that of the coupled run, except that the near-bottom temperature in the uncoupled run was colder than the data obtained from the coupled model run. Figure S2 is similar to Figure 2 in the main text but shows the uncoupled run. Note that the air temperature, prescribed as the forcing, was the same for both coupled and uncoupled runs and was thus not shown in 15 Figure S2. It shows that in most years (except for 2018), the water temperature of the uncoupled model run was underestimated at the bottom. The difference between the MARNET data and the model reached 2 ~ 3°C.

Figure S3 illustrates the spatial distribution of ϕ in each month of 2018 for an uncoupled model run. It shows a similar annual cycle of ϕ as that observed in Figure 7 of the main text. The southern North Sea become stratified from mid-spring and reached a maximum from late July to August. A clear division existed around the 50 m isobath. The water column became mixed in the 20 southern part after September, whereas north of this contour the water column was still stratified until November. Compared to the model run in which NEMO was coupled with WAM, the ϕ of the uncoupled run was larger in the entire southern North Sea domain from March to November. During the summer period (Jun to August), the maximum ϕ exceeded 1100 J m⁻³, which

was approximately 40% higher than that obtained in the coupled model run. Differences between the two runs were hardly observed in the winter period since the water column was well mixed.

25 Figure S4 is similar to that of Figure 8 in the main text but for the uncoupled run. Like the coupled model run, ϕ presents interannual variations in the southern North Sea. The degree of stratification was weaker than the multiyear mean in 2011, 2012, 2015 and 2017 (mainly in the eastern part), while it was stronger in 2013, 2014 and 2018. However, compared to the results of the coupled model run, the interannual variation was larger south of the 50 m isobath, especially in the area between 3-8°E. For example, in 2011 and 2017, the difference in ϕ was -200 J m^{-3} while it was -150 J m^{-3} in the coupled model
30 run. The maximum difference for ϕ was found in the south-east part of the domain, whereas in the coupled model run, the maximum interannual variation occurred near the northern boundary of the southern North Sea.

Figure S5 shows the correlation between the air temperatures and the degree of stratification (quantified with ϕ) computed from the water temperatures of the uncoupled model run. The correlation coefficient $R > 0.5$ covered the region of seasonal stratification, which was consistent with that of the coupled model run. In the Norwegian Trench and the Dutch Coast, where
35 stratification was not caused by the thermocline, R illustrated a spatial pattern similar to that of the coupled model run. However, in the uncoupled run, the permanent mixed region was smaller. Near the Wadden Sea, the water column was stratified with $0 < R < 0.4$. Meanwhile, a larger area with a negative R was obtained in the German bight region.

Figure S6 is similar to Figure 10 in the main text, but for the uncoupled model run. Although the overall spatial pattern of the ratio “ r ” was similar to that of the coupled model run, its value is smaller. In the seasonally stratified region ($R > 0.6$), r
40 was approximately 0. In other words, the number of stratification days during the entire warming season (May to August) had no interannual variation. Note that in the uncoupled model run, the seasonal stratification was also dominant in part of the area south of the 50 m isobath, especially around the Dogger Bank station. The region in which a large r occurred was mostly near the southern coast of the North Sea, with the maximum value located west to the Danish Wadden Sea.

Like Figure 11 in the main text, Figure S7 illustrates the ratio between the change in stratification days and the change
45 in intensive air temperature incline. The maximum ratio was observed outside the Rhine estuary near the Belgium coast and next to the permanently mixed region. This was caused by the reduced interannual variation in stratification. Rather than heat exchange at the water surface, the stratification in this region is generated by the fresh water input from the Rhine River. The stratification becomes stronger and more stable due to the absence of turbulent mixing by the waves.

This was also clear when comparing the gradient R_i of the uncoupled model run (Figure S8) with that of the coupled model
50 run (see Figure 12 in the main text). For both 2015 and 2018, $\log_{10}R_i$ had a larger value and lasted longer than that it in the coupled run. In the Northsea Mid, stable stratification lasted even until the end of the year. However, similar to the coupled run, $\log_{10}R_i > 1$ mainly occurred within 45 m water depth. At Dogger Bank and NSB III, $\log_{10}R_i > 1$ was observed from the beginning of June until October in both 2015 and 2018. This was much larger than the value obtained in the coupled model run. Moreover, large R_i (i.e., $\log_{10}R_i > 1$) reached 10 m above the bottom. At the NSB III station, the small R_i in 2015 implied
55 a homogeneous water column in the whole year. In 2018, a large R_i was obtained from mid-May and June 25 m above the bottom and from July until early September 20 m above the bottom. In this year, stratification developed in July and August in Fino-1.

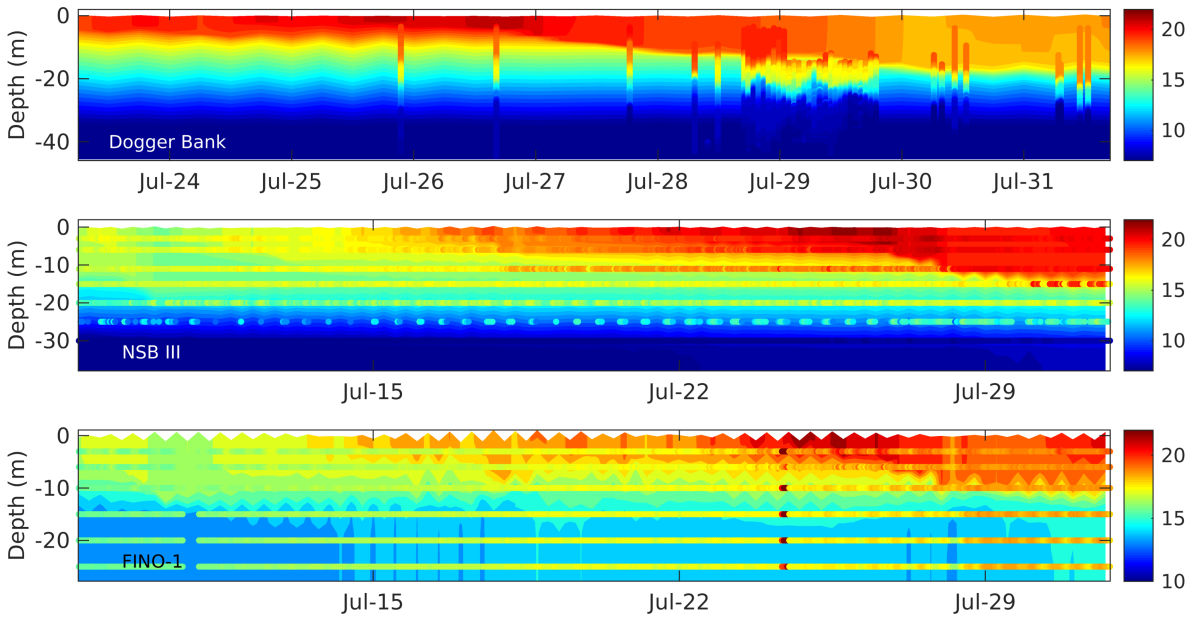


Figure S1. Comparing water temperatures (in °C) in July 2017 of the in-situ observations with the results from the uncoupled circulation model.

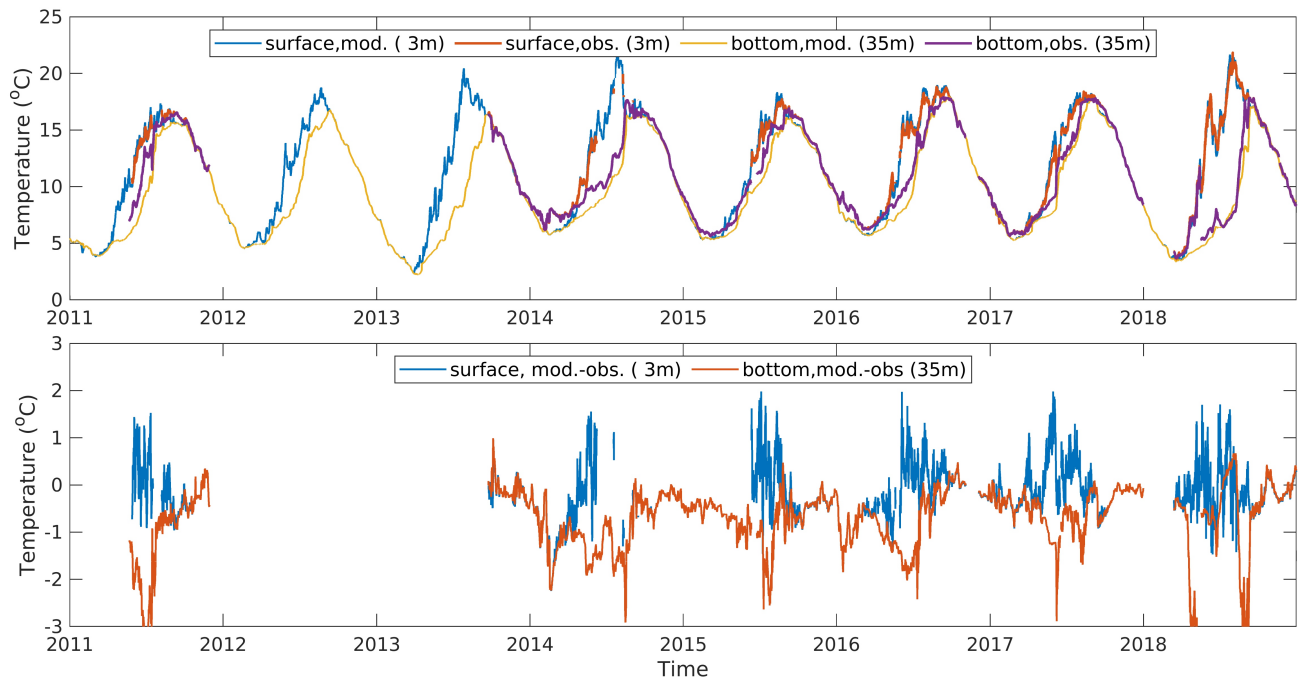


Figure S2. Upper panel: Interannual variation in temperature in the water surface and bottom of the observations (obs.) and the simulations (mod.). Lower panel: The differences between modelled seawater temperature and the observed temperature in the water surface and bottom.

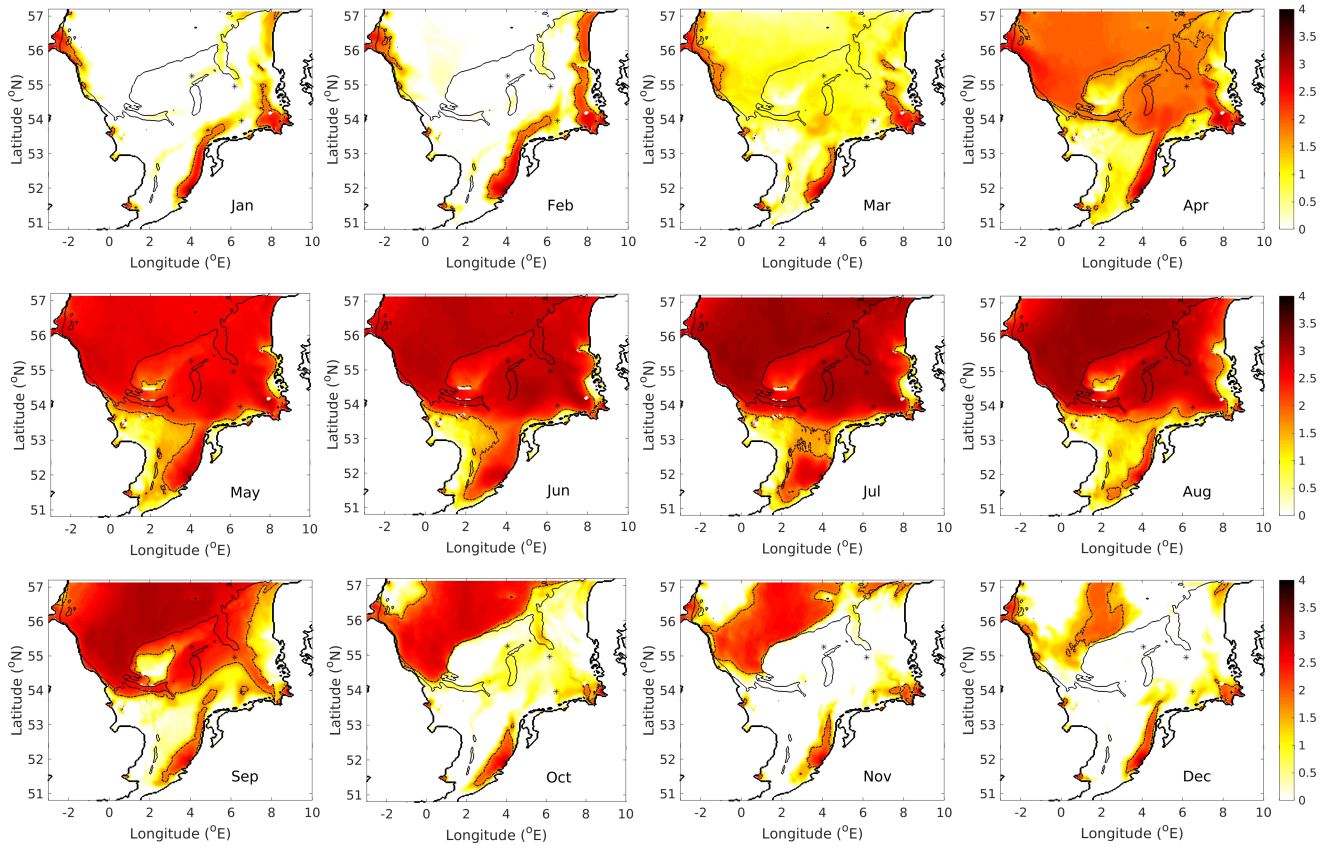


Figure S3. Evolution of the potential energy anomaly ϕ (J m^{-3} on a log10 scale) in 2018. Dashed line indicates $\phi = 50 \text{ J m}^{-3}$. The water column is considered to be stratified when ϕ is above this value. Thin black lines indicate the location of 50 m depth.

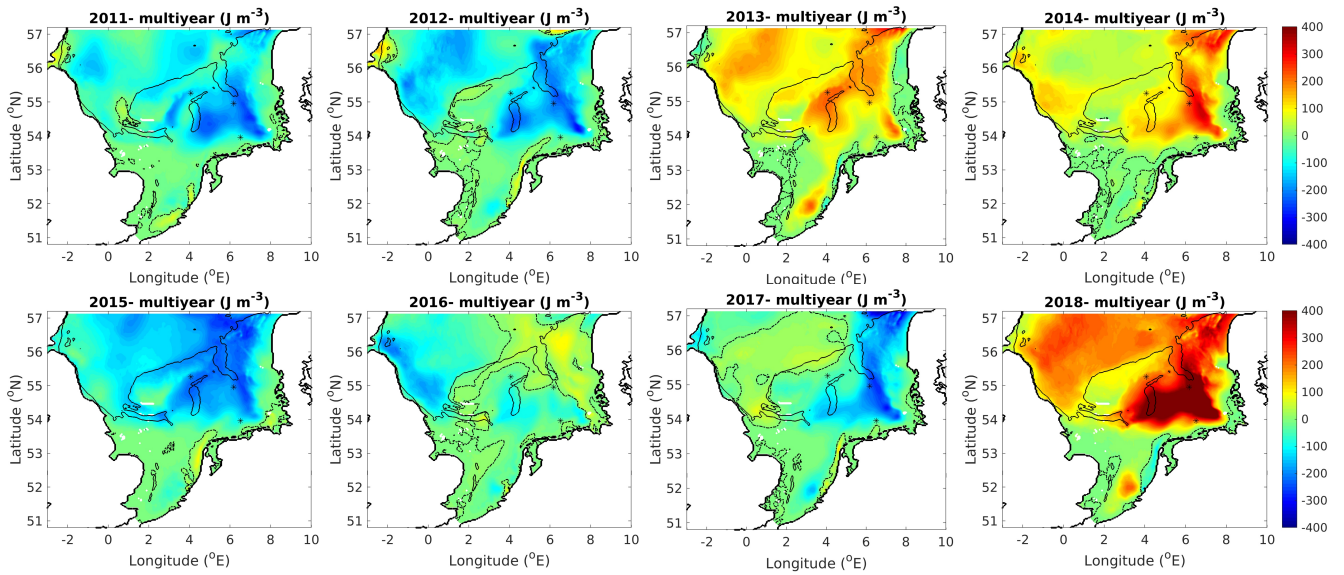


Figure S4. Difference in three-monthly mean potential energy anomaly (J m^{-3}) between a specific year and the multiyear mean. Dashed line indicates $\phi = 50 \text{ J m}^{-3}$. Thin black lines indicate the location of 50 m depth.

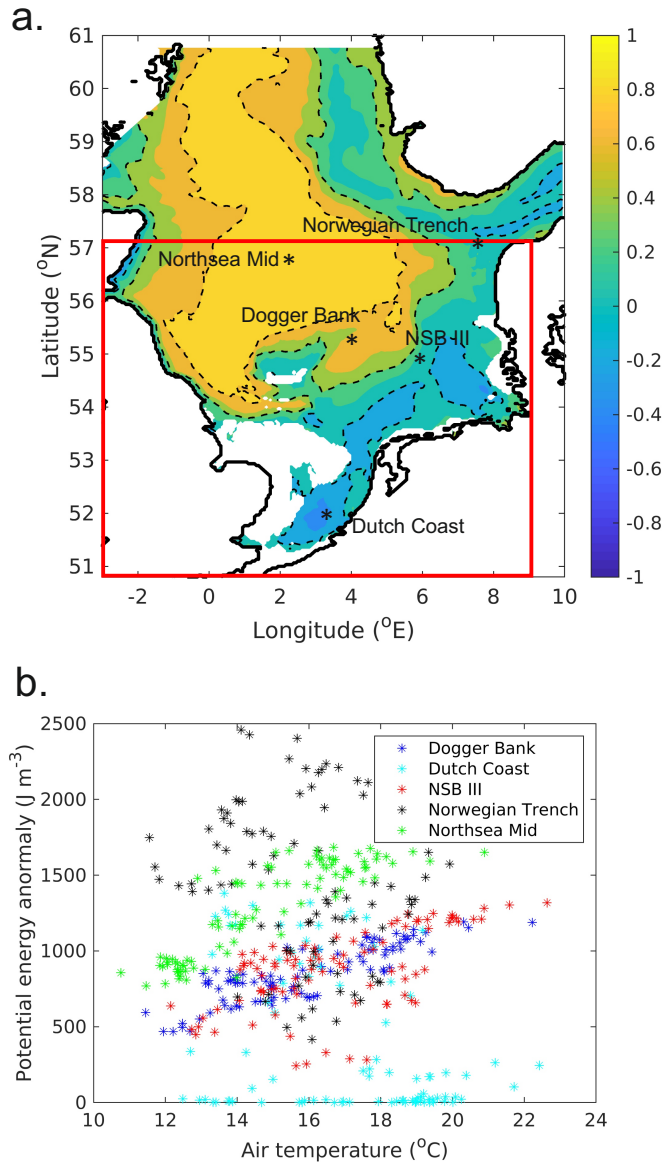


Figure S5. (a): Computed correlation coefficient ‘R’ between the air temperature and the potential energy anomaly for summer time 2018. Note that the area with no stratification ($\phi < 50 \text{ J m}^{-3}$) is cut off. Dashed contours indicate $R = 0, 0.4$ and 0.8 . (b): The relationship between the air temperature and the potential energy anomaly in the different regimes of the North Sea. The locations are illustrated in (a). The red frame indicates the region of the southern North Sea.

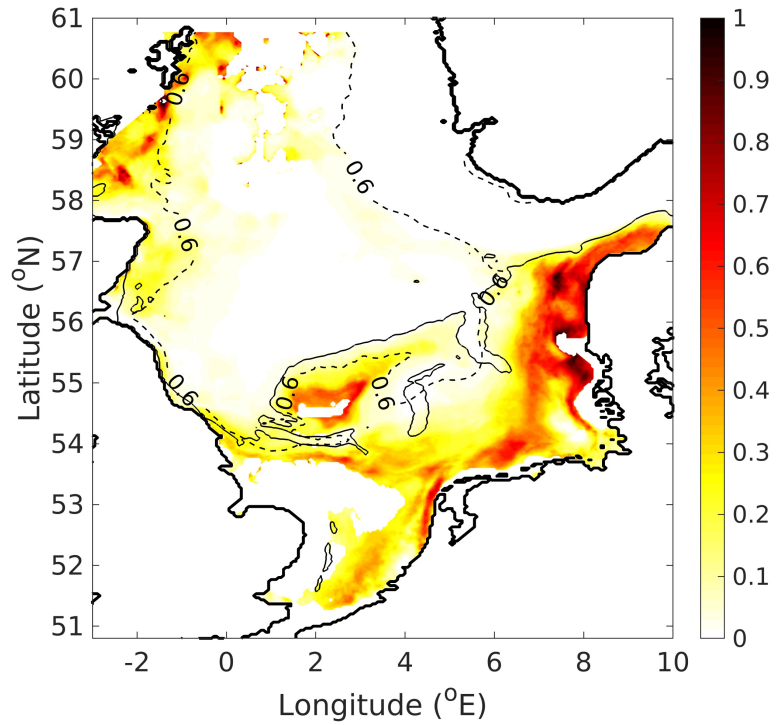


Figure S6. The ratio between the number of days when the water was stratified and the number of days in MHW events. The contour line with the value 0.6 indicate the area that correlation coefficient ' $R = 0.6$ ' between the air temperature and the potential energy anomaly for the summer time of the multiyear mean.

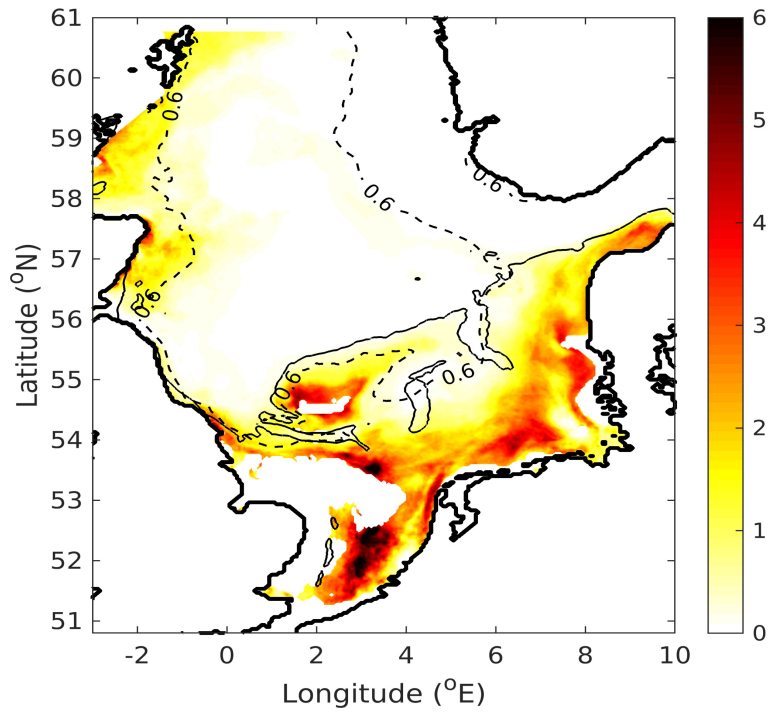


Figure S7. The ratio between the number of days when the water is stratified and the number of days during intensive air temperature incline. The contour line with a value of 0.6 indicates the area with a correlation coefficient ' $R = 0.6$ ' between the air temperature and the potential energy anomaly for summer time of the multiyear mean.

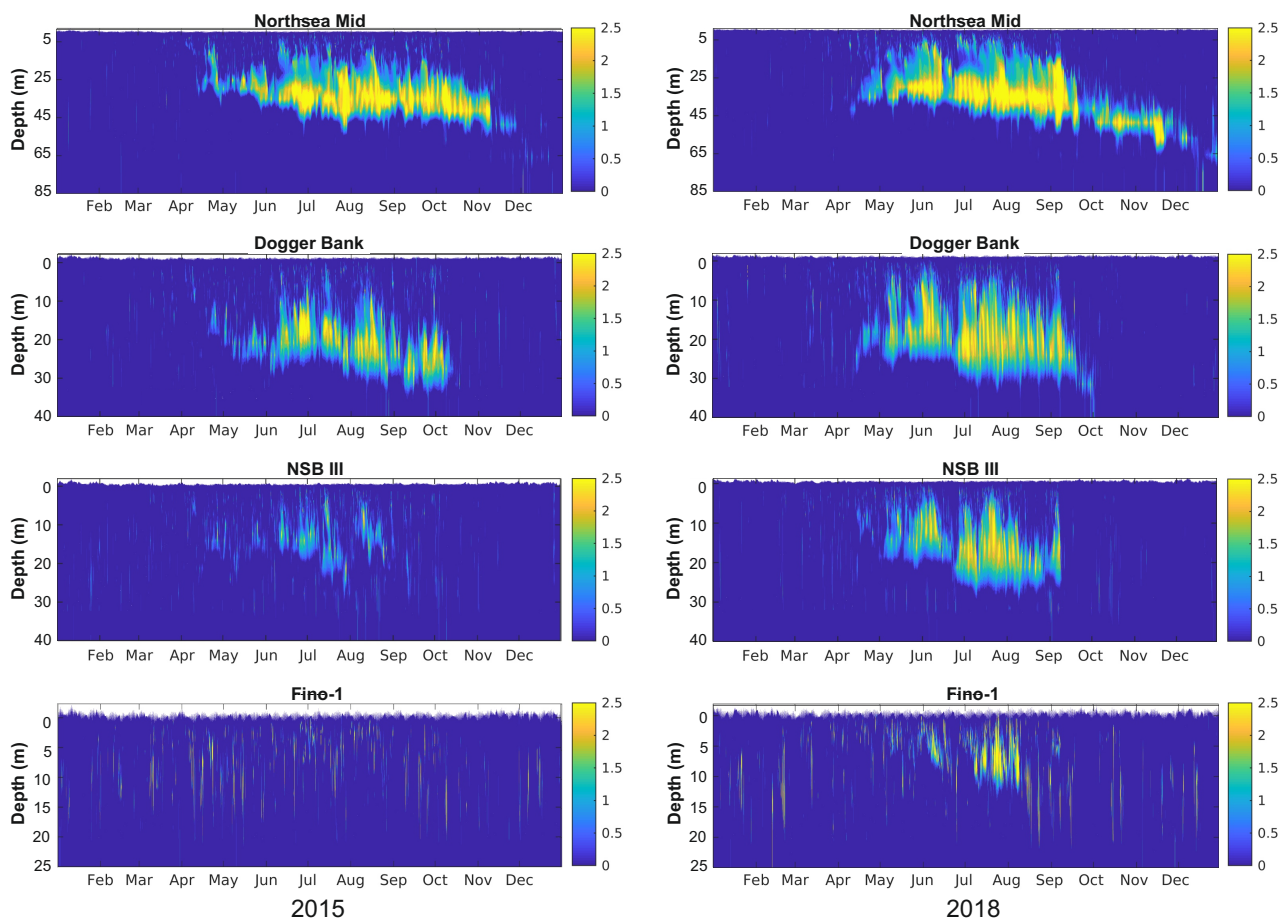


Figure S8. Gradient Ri for 2015 (left column) and 2018 (right column) at Northsea Mid, Dogger Bank, NSB III and Fino-1 on a log₁₀ scale.